

Exceptional Points of Degeneracy and Branch Points for Transmission-Line Problems – Linear Algebra and Bifurcation Theory Perspectives

George W. Hanson*

*Department of Electrical Engineering and Computer Science,
University of Wisconsin-Milwaukee, 3200 N. Cramer St., Milwaukee, Wisconsin 53211, USA*

Alexander B. Yakovlev†

Department of Electrical Engineering, The University of Mississippi, University, Mississippi 38677, USA

Mohamed Othman‡ and Filippo Capolino§

*Department of Electrical Engineering and Computer Science,
University of California-Irvine, Irvine, California 92697-2625, USA*

(Dated: April 11, 2018)

We demonstrate several new aspects of exceptional points of degeneracy (EPD) pertaining to propagation in two uniform coupled transmission-line structures. We describe an EPD using two different approaches – by solving an eigenvalue problem based on the system matrix, and as a singular point from bifurcation theory, and the link between these two disparate viewpoints. Cast as an eigenvalue problem, we show that eigenvalue degeneracies are always coincident with eigenvector degeneracies, so that all eigenvalue degeneracies are implicitly EPDs in two uniform coupled transmission lines. Furthermore, we discuss in some detail the fact that EPDs define branch points (BPs) in the complex-frequency plane; we provide simple formulas for these points, and show that parity-time (PT) symmetry leads to real-valued EPDs occurring on the real-frequency axis. We discuss the connection of the linear algebra approach to previous waveguide analysis based on singular points from bifurcation theory, which provides a complementary viewpoint of EPD phenomena, showing that EPDs are singular points of the dispersion function associated with the fold bifurcation. This provides an important connection of various modal interaction phenomena known in guided-wave structures with recent interesting effects observed in quantum mechanics, photonics, and metamaterials systems described in terms of the EPD formalism.

I. INTRODUCTION

When propagation in a coupled-waveguide system is described in terms of a system matrix, exceptional points of degeneracy are points in the parameter space of such a system at which simultaneous eigenvalue and eigenvector degeneracies occur [1]. Interest in EPDs has recently risen due to Parity-Time (PT) symmetric systems, wherein non-Hermitian Hamiltonians can nevertheless exhibit real spectra, representing physical observables. PT-symmetry has led to a range of interesting phenomena in quantum mechanics and photonic systems [2–7], and in metamaterials research [8–11], with applications to cloaking, negative refraction, imaging, field transformation, and sensing, among others. In a system whose evolution is described with a system matrix, EPDs are associated with a Jordan block, corresponding to a deficient (incomplete) set of eigenfunctions, and algebraically growing solutions of generalized (associated) eigenvectors at the EPD. Moreover, in the vicinity of EPDs, by virtue of small detuning, eigenvalues exhibit unconventional perturbations following a fractional power-law ex-

pansion in the perturbation parameters [12].

It is important to point out that EPDs are manifest in the parameter space of a system's eigenstates' temporal evolution (e.g., such as certain coupled resonators with loss and gain), or of a system's eigenstates' spatial evolution. This latter case represents the evolution of eigenwaves in a given spatial direction, such as in a multimode waveguide with prescribed loss and gain, which is investigated in this paper, where the multimode waveguide is a pair of uniform coupled transmission lines. Some of the earliest examples of EPDs have been also observed in structures with spatial periodicity which are explored, for instance, in [13–16], such as those exhibiting degenerate band edges or stationary inflection points. Although EPDs are usually viewed from a linear algebra standpoint, and are associated with systems described by matrices with Jordan blocks [1, 13], it has been observed that they also represent points in configuration space where multiple branches of spectra connect, and are linked to branch points in the space of control variables [17, 18].

In this work, we consider a coupled uniform transmission-line system, recently examined in [19], and demonstrate several new aspects of EPDs in these systems. Specifically, we stress that for a coupled uniform transmission line, eigenvalue degeneracies always result in eigenvector degeneracies, such that all eigenvalue degeneracies represent EPDs. We derive closed-form ex-

* george@uwm.edu

† yakovlev@olemiss.edu

‡ mothman@uci.edu

§ f.capolino@uci.edu

pressions for the branch-point singularities/EPDs using bifurcation theory. We show and discuss in detail the connection of EPDs with previous work on fold-point and branch-point singularities in waveguiding systems [20–28] associated with mode degeneracies and mode interactions, which provides a complementary viewpoint for understanding EPDs.

II. COUPLED TRANSMISSION-LINE FORMULATION

We consider two uniform coupled transmission lines (CTLs) as depicted in Fig. 1.

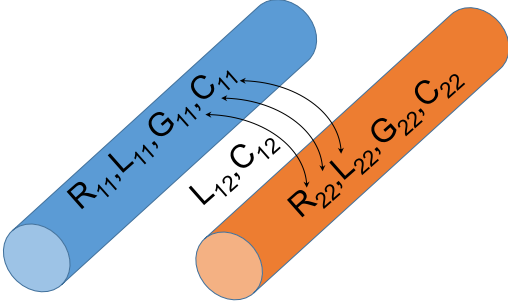


Figure 1. Two coupled transmission lines with mutual capacitive and inductive coupling, invariant along z . They exhibit EPDs under certain conditions described in the paper.

We refer to the formulation given in [19] for the analysis of eigenwaves propagating along the z -direction in a CTL (the $e^{i\omega t}$ time-harmonic evolution is implicitly assumed). Here we summarize the mathematical steps carried out to obtain the eigenwaves supported by such a guiding system. The CTL equations for a two-line network consisting of uniform transmission lines are given by the telegraphers equations [29, 30]

$$\frac{d\mathbf{V}(z)}{dz} = -\underline{\underline{\mathbf{Z}}}\mathbf{I}(z), \quad \frac{d\mathbf{I}(z)}{dz} = -\underline{\underline{\mathbf{Y}}}\mathbf{V}(z) \quad (1)$$

where the voltage and current are 2-dimensional vectors, $\mathbf{V}(z) = [V_1(z) \ V_2(z)]^T$ and $\mathbf{I}(z) = [I_1(z) \ I_2(z)]^T$, whereas $\underline{\underline{\mathbf{Z}}}$ and $\underline{\underline{\mathbf{Y}}}$ are 2×2 matrices,

$$\underline{\underline{\mathbf{Z}}}(\omega) = \begin{bmatrix} Z_{11} & Z_{12} \\ Z_{21} & Z_{22} \end{bmatrix}, \quad \underline{\underline{\mathbf{Y}}}(\omega) = \begin{bmatrix} Y_{11} & Y_{12} \\ Y_{21} & Y_{22} \end{bmatrix}, \quad (2)$$

where the off-diagonal elements represent coupling between the two transmission lines. Furthermore, the per-unit-length series impedance and shunt admittance matrices are given by $\underline{\underline{\mathbf{Z}}} = i\omega\underline{\underline{\mathbf{L}}} + \underline{\underline{\mathbf{R}}}$ and $\underline{\underline{\mathbf{Y}}} = i\omega\underline{\underline{\mathbf{C}}} + \underline{\underline{\mathbf{G}}}$, where $\underline{\underline{\mathbf{R}}}$, $\underline{\underline{\mathbf{G}}}$, $\underline{\underline{\mathbf{L}}}$, and $\underline{\underline{\mathbf{C}}}$ are matrices of the per-unit-length distributed CTL parameters, assumed nondispersive for simplicity. The matrices $\underline{\underline{\mathbf{L}}}$ and $\underline{\underline{\mathbf{C}}}$ are positive definite and symmetric [29, 30], and the off-diagonal entries of $\underline{\underline{\mathbf{C}}}$

and $\underline{\underline{\mathbf{G}}}$ are negative. In general $\underline{\underline{\mathbf{R}}}$ and $\underline{\underline{\mathbf{G}}}$ are positive definite if they represent losses (no gain), and in the following they are assumed to be diagonal for simplicity. In addition, note also that the per-unit-length impedance and admittance matrices may possess cutoff capacitance and inductance terms, respectively, as done in Ch. 7 in [31], and also in [32] to model waveguide cutoff. Since we do not investigate cutoff related degeneracies, we simply ignore these terms in the CTL formulations above.

A. EPD from a Linear Algebra Perspective

Decoupling (1), we obtain two second-order wave equations for the voltage and current vectors

$$\frac{d^2\mathbf{V}(z)}{dz^2} = \underline{\underline{\mathbf{Z}}}\underline{\underline{\mathbf{Y}}}\mathbf{V}(z), \quad \frac{d^2\mathbf{I}(z)}{dz^2} = \underline{\underline{\mathbf{Y}}}\underline{\underline{\mathbf{Z}}}\mathbf{I}(z). \quad (3)$$

The two systems lead to the same wavenumber solutions though in general, $\underline{\underline{\mathbf{Z}}}$ and $\underline{\underline{\mathbf{Y}}}$ do not necessarily commute; one common exception is for lossless lines in a homogeneous environment characterized by μ, ε , in which case $\underline{\underline{\mathbf{Z}}}\underline{\underline{\mathbf{Y}}} = -\omega^2\mu\varepsilon\underline{\underline{\mathbf{1}}}$, where $\underline{\underline{\mathbf{1}}}$ is the 2×2 identity matrix. Alternatively, one may form a four-dimensional state vector $\Psi(z) = [V_1(z) \ V_2(z) \ I_1(z) \ I_2(z)]^T$, leading to

$$\frac{d}{dz}\Psi(z) = -i\underline{\underline{\mathbf{M}}}(\omega)\Psi(z) \quad (4)$$

where

$$\underline{\underline{\mathbf{M}}}(\omega) = \begin{bmatrix} \underline{\underline{\mathbf{0}}} & -i\underline{\underline{\mathbf{Z}}} \\ -i\underline{\underline{\mathbf{Y}}} & \underline{\underline{\mathbf{0}}} \end{bmatrix}. \quad (5)$$

Assuming that the transmission line is invariant along z , the homogeneous solutions to (3) and (4) are found to be in the form $\Psi(z) \propto e^{-ikz}$ with k being the wavenumber. As such, (3) and (4) become

$$\begin{aligned} -(\underline{\underline{\mathbf{Z}}}\underline{\underline{\mathbf{Y}}})(\omega)\mathbf{V}(z) &= k^2\mathbf{V}(z), \\ -(\underline{\underline{\mathbf{Y}}}\underline{\underline{\mathbf{Z}}})(\omega)\mathbf{I}(z) &= k^2\mathbf{I}(z), \\ \underline{\underline{\mathbf{M}}}(\omega)\Psi(z) &= k\Psi(z). \end{aligned} \quad (6)$$

Note that the first two equations in (6) have two eigenvalues k^2 (and both signs of k are possible), whereas the third equation in (6) has four eigenvalues k . All three eigenvalue problems lead to the same four eigenvalues, and encompass the same physics, which is thoroughly explained in [19]. Here, we wish to make several new observations about these eigenproblems from two different but complementary perspectives, which opens up new ways for utilizing such EPDs and conceiving new operational principles for a variety of microwave devices. For simplicity, we assume reciprocity, i.e., $Y_{21} = Y_{12}$ and $Z_{21} = Z_{12}$.

We denote the algebraic multiplicity for eigenvalues λ (i.e., the order of the eigenvalue degeneracy) as $m(\lambda)$. The geometric multiplicity of the eigenvalue (the span of the eigenvector space associated with the eigenvalue) is denoted as $l(\lambda)$. We make the following observations related to EPDs:

1. For the systems of CTLs considered above, when an EPD occurs one has $m(\lambda) > l(\lambda)$, i.e., all degenerate eigenvalues have a deficient eigenspace, and the matrices $\underline{\mathbf{M}}, \underline{\mathbf{Z}}\underline{\mathbf{Y}}, \underline{\mathbf{Y}}\underline{\mathbf{Z}}$ cannot be diagonalized (except for the trivial degeneracy at $k=0$ and in uncoupled lines). In particular, for the two uniform CTLs considered here, EPDs are associated with $l(\lambda) = 2$, and $m(\lambda) = 1$.
2. EPDs imply the presence of square-root branch points in the complex-frequency plane. As such, these complex-frequency plane singularities are generally unavailable for monochromatic problems, but may be accessed in certain pulse shaping scenarios [33–35].
3. The analysis of EPD from a linear algebra perspective can analogously be studied as fold singularities of mappings in bifurcation theory.
4. PT-symmetric conditions lead to EPDs on the real-frequency axis, and, thus, to physically observable phenomena in monochromatic problems.

In the following, we examine the aforementioned statements and provide analytical expressions for the eigenvalues and eigenvectors to reveal the origin of EPDs and their relation to eigenvalue and eigenvector degeneracies and branch points. In Section II B we examine EPDs from a different prospective, that of bifurcation theory.

We first consider the 2×2 eigenvalue problem in (6); $-\underline{\mathbf{Z}}\underline{\mathbf{Y}}$ having eigenvalues $k_{1,2}^2$ and regular voltage eigenvectors $\mathbf{V}_{1,2}$, obtained analytically as

$$k_n^2 = \frac{1}{2}(-T + (-1)^n D), \quad \mathbf{V}_n = \begin{bmatrix} -\frac{1}{2N_1}(N_2 + (-1)^n D) \\ 1 \end{bmatrix} \quad (7)$$

where $n = 1, 2$, then $N_1 = Y_{11}Z_{12} + Y_{12}Z_{22}$, $N_2 = -Y_{11}Z_{11} + Y_{22}Z_{22}$ and

$$D = \sqrt{T^2 - 4\det(\underline{\mathbf{Z}}\underline{\mathbf{Y}})}. \quad (8)$$

The trace T and determinant of $\underline{\mathbf{Z}}\underline{\mathbf{Y}}$ are given by

$$T = \text{Tr}(\underline{\mathbf{Z}}\underline{\mathbf{Y}}) = 2Y_{12}Z_{12} + Y_{22}Z_{22} + Y_{11}Z_{11}, \quad (9)$$

$$\det(\underline{\mathbf{Z}}\underline{\mathbf{Y}}) = (Y_{11}Y_{22} - Y_{12}^2)(Z_{11}Z_{22} - Z_{12}^2). \quad (10)$$

For the $-\underline{\mathbf{Y}}\underline{\mathbf{Z}}$ formulation in (6), everything is analogous; the same eigenvalues are obtained, and the regular current $\mathbf{I}_{1,2}$ eigenvectors are retrieved using (7) by replacing $N_1 \rightarrow Y_{22}Z_{12} + Y_{12}Z_{11}$.

It is obvious that, without considering the trivial eigenvalue degeneracy at $k = 0$, eigenvalue degeneracies occur when $D = 0$, and, moreover, from (7) it is clear that at this point eigenvectors are also degenerate; $m(k^2) = 2$ and $l(k^2) = 1$ since $\mathbf{V}_1 = \mathbf{V}_2$.

For the formulation in (6) involving the 4×4 matrix $\underline{\mathbf{M}}$, one finds the four eigenvalues and regular eigenvectors as

$$k_n = (\pm) \frac{1}{\sqrt{2}} \sqrt{-T + \nu_n D}, \quad (11)$$

$$\Psi_n = \begin{bmatrix} (\pm) i \frac{\sqrt{-T + \nu_n D}}{\sqrt{2}} \frac{-N_2 - \nu_n D}{N_3 - \nu_n Y D} \\ (\pm) i \frac{2\sqrt{-T + \nu_n D}}{\sqrt{2}} \frac{N_1}{N_3 - \nu_n Y_{12} D} \\ \frac{(-N_2 - \nu_n D)Y_{11} + 2Y_{12}N_1}{N_3 - \nu_n Y_{12} D} \\ 1 \end{bmatrix}, \quad (12)$$

where the $+$ sign in front is for $n = 1, 2$, the $-$ sign in front is for $n = 3, 4$, $\nu_n = (-1)^n$, $N_3 = Y_{11}(Y_{12}Z_{11} + 2Y_{22}Z_{12}) + Y_{12}Y_{22}Z_{22}$, and again both eigenvalues and eigenvectors become simultaneously degenerate when $D = 0$, and $m(\pm k) = 2 > l(\pm k) = 1$.

Therefore, excepting the case of uncoupled identical lines [36] and $k = 0$, for all system descriptions in (6) eigenvector degeneracies are simultaneous with eigenvalue degeneracies. Thus, these simultaneous eigenvalue and eigenvector degeneracies are, by definition, an EPD, where $k = \pm k_e$ with $k \equiv \sqrt{-T}/\sqrt{2}$. Indeed at such points the matrices in (6) are deficient and cannot be diagonalized because there are not enough eigenvectors to form a complete basis. This proves Item 1 above. From the above analysis, Item 2 is also demonstrated, since $D = D(\omega)$ clearly represents a square-root type branch point in the complex- ω plane.

Conditions for EPDs were also presented in [19]; here we briefly comment on those and the connection with the condition $D = 0$. In [19], it was shown that the conditions

$$T = \text{Tr}(\underline{\mathbf{Z}}\underline{\mathbf{Y}}) = -2k^2, \quad (13)$$

$$\det(\underline{\mathbf{Z}}\underline{\mathbf{Y}}) = k^4, \quad (14)$$

are necessary for an eigenvalue degeneracy (and so, in fact, are necessary and sufficient for an EPD as described previously, excepting $k = 0$ and uncoupled lines). These two conditions combined yield $\det(\underline{\mathbf{Z}}\underline{\mathbf{Y}}) = T^2/4$, which is the condition under which $D = 0$.

Furthermore, when, e.g., $\underline{\mathbf{M}}$ is similar to a diagonal matrix (away from the EPD) it can be written in the form

$$\underline{\mathbf{M}} = \underline{\mathbf{U}}\underline{\mathbf{\Lambda}}\underline{\mathbf{U}}^{-1} \quad (15)$$

where $\underline{\mathbf{U}}$ is a 4×4 matrix representing the similarity transformation of $\underline{\mathbf{M}}$ that brings it to a diagonal form, and $\underline{\mathbf{\Lambda}}$ is a diagonal matrix whose diagonal entries are the eigenvalues k_n in (11). It was shown in [19] that the condition $\det(\underline{\mathbf{U}}) = 0$ provides necessary and sufficient conditions for an eigenvector degeneracy (at which point the regular eigenvectors must be augmented with associated eigenvectors, and, rather than a diagonal form, the simplest matrix representation is given by the Jor-

dan canonical form [37]). Forming

$$\det(\underline{\mathbf{U}}) = -16 \frac{Y_{11}}{N_2^3} D^2 (Y_{12}Z_{22} + Y_{11}Z_{12}) \sqrt{T^2 - D^2} = 0 \quad (16)$$

it is observed that $\det(\underline{\mathbf{U}}) = 0$ occurs when $D = 0$ (or when $Y_{12}Z_{22} + Y_{11}Z_{12} = 0$, which seems to not be of practical interest, and note that $D = T$ cannot be true since, using (8), it would hold only if $\det(\underline{\mathbf{Z}}\underline{\mathbf{Y}}) = 0$, which is not true). Alternatively, assuming a similarity transformation analogous to that in (15) but that diagonalizes the 2×2 matrix $-\underline{\mathbf{Z}}\underline{\mathbf{Y}}$,

$$\det(\underline{\mathbf{U}}) = -\frac{D}{Y_{11}Z_{12} + Y_{12}Z_{22}} \quad (17)$$

which again occurs at $D = 0$. Therefore, the previously stated conditions in [19] are, for uniform CTLs modeled by nondispersive $\underline{\mathbf{R}}$, $\underline{\mathbf{G}}$, $\underline{\mathbf{L}}$, and $\underline{\mathbf{C}}$ parameters, alternative ways of stating the $\bar{D} = 0$ EPD condition.

Puiseux series. In what follows, it will be useful to cast the eigenvalue problems (6) in the form

$$H(k, \omega) = \det(\mathbf{A}(\omega, \boldsymbol{\xi}) - k\mathbf{1}) = 0 \quad (18)$$

where $\boldsymbol{\xi}$ is the vector of geometrical and material parameters of the system, and $\mathbf{1}$ is the identity matrix. In particular, in the following, all the partial derivatives in ω could be substituted with partial derivatives in $\boldsymbol{\xi}$ and analogous conclusions would be reached relative to the dispersion diagram $(k, \boldsymbol{\xi})$ and associated BPs. In (18), the matrix \mathbf{A} represents either the 2×2 system for which $\underline{\mathbf{A}} = -\underline{\mathbf{Z}}\underline{\mathbf{Y}}$, or $\underline{\mathbf{A}} = -\underline{\mathbf{Y}}\underline{\mathbf{Z}}$ (in which case the eigenvalue is k^2 rather than k) or the 4×4 system $\underline{\mathbf{A}} = \underline{\mathbf{M}}$. In the following we suppress the dependence on $\boldsymbol{\xi}$. The condition (18) leads to

$$k^4 + k^2 \text{Tr}(\underline{\mathbf{A}}) + \det(\underline{\mathbf{A}}) = 0, \quad (19)$$

which is also given in [19]. Denoting derivatives as

$$H_\varsigma^{(m)}(k_e, \omega_e) = \left. \frac{\partial^{(m)} H(k, \omega)}{\partial \varsigma^m} \right|_{(k_e, \omega_e)}, \quad (20)$$

for $\varsigma = k, \omega$, an m th-order eigenvalue degeneracy (i.e., an m th-order root of $H(k, \omega)$) will satisfy

$$H(k_e, \omega_e) = H'_k(k_e, \omega_e) = \dots = H_k^{(m-1)}(k_e, \omega_e) = 0, \quad (21)$$

$$H_k^{(m)}(k_e, \omega_e) \neq 0, \quad (22)$$

where k_e is the degenerate wavenumber and ω_e is the frequency at which the wavenumbers become degenerate. For a second-order EPD, the condition $H'_k(k, \omega) = 0$ is

$$k(T + 2k^2) = 0, \quad (23)$$

which is equivalent to the trace condition (13) for $k \neq 0$, and leads to $k = \pm\sqrt{-T}/\sqrt{2}$, consistent with the general

eigenvalue at the EPD. As described briefly in [19] but of more direct importance here, the eigenvalues of the CTL at such a degeneracy can be written as a convergent Puiseux series [12, 38]

$$k_n(\omega) = k_e + \alpha_1 \zeta^n (\omega - \omega_e)^{\frac{1}{m}} + \sum_{p=2}^{\infty} \alpha_p (\zeta^n (\omega - \omega_e)^{\frac{1}{m}})^p \quad (24)$$

for $n = 0, 1, 2, \dots, m-1$, where $\zeta = e^{i\frac{2\pi}{m}}$. The first-order coefficient is given by

$$\alpha_1 = \left(-\frac{H'_\omega(k_e, \omega_e)}{\frac{1}{m!} H_k^{(m)}(k_e, \omega_e)} \right)^{\frac{1}{m}}. \quad (25)$$

The Puiseux series is a direct consequence of the Jordan Block form (see for example page 65 in [12]) hence it is always relevant in systems that exhibit an EPD to describe the eigenvalue perturbation away from the EPD. Applying the fractional power expansion (24) to the 2nd order EPD in the uniform CTL above, and ignoring expansion terms with order equal or higher than $\omega - \omega_e$, one arrives at

$$k(\omega) \simeq k_e \pm \alpha_1 \sqrt{\omega - \omega_e} + O(\omega - \omega_e). \quad (26)$$

The first two terms in (26) show the occurrence of the branch-point singularity in the complex-frequency plane, resulting from the square-root function. Associated with this series is the condition [38]

$$H'_\omega(k_e, \omega_e) \neq 0, \quad (27)$$

and so the first-order coefficient α_1 is nonzero. An important aspect of the Puiseux series is that it provides the characteristic form of the solution in the vicinity of the EPD, as shown later in relation to Fig. 2. Regarding Statement 3, the conditions (21)-(22), and (27) will be reconsidered in Section II B from the viewpoint of singularity and bifurcation theory.

Jordan Block and Generalized Eigenvectors. At an EPD in a uniform 2-CTL, the eigenvalue degeneracy corresponds to an eigenvector degeneracy as we have previously discussed. This can be also shown by noticing that when the eigenvalues of a 2×2 system matrix, as in the first two systems in (6), are identical then it is either proportional to an identity matrix (hence with two independent eigenvectors) or otherwise it must be proportional to a 2×2 Jordan block (that exhibit the eigenvector degeneracy). For the 4×4 system matrix $\underline{\mathbf{M}}$ as in the third system in (6) the situation is more involved. At an EPD the system matrix $\underline{\mathbf{M}}$ is similar to a matrix containing two Jordan blocks as

$$\underline{\mathbf{M}} = \underline{\mathbf{U}} \begin{bmatrix} \underline{\mathbf{J}}_+ & \underline{\mathbf{0}} \\ \underline{\mathbf{0}} & \underline{\mathbf{J}}_- \end{bmatrix} \underline{\mathbf{U}}^{-1}, \quad \underline{\mathbf{J}}_{\pm} = \begin{bmatrix} \pm k_e & 1 \\ 0 & \pm k_e \end{bmatrix} \quad (28)$$

where $\underline{\mathbf{U}}$ is a 4×4 matrix constituting a similarity transformation and containing the generalized eigenvectors of $\underline{\mathbf{M}}$ namely $\underline{\mathbf{S}} = [\Psi_1 \mid \Psi_1^g \mid \Psi_3 \mid \Psi_3^g]$ that are constructed through the Jordan chain procedure ([19], [39], see also [40] for the differential operator case)

$$(\underline{\mathbf{M}} - k_e \underline{\mathbf{1}}) \Psi_1 = 0, \quad (\underline{\mathbf{M}} - k_e \underline{\mathbf{1}}) \Psi_1^g = \Psi_1 \quad (29)$$

$$(\underline{\mathbf{M}} + k_e \underline{\mathbf{1}}) \Psi_3 = 0, \quad (\underline{\mathbf{M}} + k_e \underline{\mathbf{1}}) \Psi_3^g = \Psi_3 \quad (30)$$

with Ψ_1 and Ψ_1^g being the regular and generalized eigenvectors associated with the wavenumber k_e at the second-order EPD, and similarly Ψ_3 and Ψ_3^g are the regular and generalized eigenvectors associated with the wavenumber $-k_e$.

We consider the general solution of (4) subject to an initial condition at an arbitrary $z = z_0$ given by $\Psi(z_0) = \Psi_0$. Its general and unique solution is given by

$$\begin{aligned} \Psi(z) &= \exp(-i\underline{\mathbf{M}}z) \Psi_0 \\ &= \underline{\mathbf{U}} \begin{bmatrix} \exp(-i\underline{\mathbf{J}}_+ z) & \underline{\mathbf{0}} \\ \underline{\mathbf{0}} & \exp(-i\underline{\mathbf{J}}_- z) \end{bmatrix} \underline{\mathbf{U}}^{-1} \Psi_0, \\ &= \underline{\mathbf{U}} \left(\begin{bmatrix} e^{-ik_e z} & -iz e^{-ik_e z} & 0 & 0 \\ 0 & e^{-ik_e z} & 0 & 0 \\ 0 & 0 & e^{+ik_e z} & iz e^{+ik_e z} \\ 0 & 0 & 0 & e^{+ik_e z} \end{bmatrix} z \right) \underline{\mathbf{U}}^{-1} \Psi_0 \end{aligned}$$

which provides growing solutions along z as $\Psi(z) \propto z e^{-ik_e z}$ discussed in [19].

B. EPD from a Theory of Singular and Bifurcation Points Perspective

Here, we address Statement 3, and connect the previous analysis with an entirely different method based on singularity and bifurcation theory [41, 42]. We consider the implicit dispersion equation (18), $H(k, \omega) = \det(\mathbf{A}(\omega) - k \mathbf{1}) = 0$. Here, $H(k, \omega)$ is more generally understood as a mapping $\mathbb{C}^2 \rightarrow \mathbb{C}$, $H(k, \omega) = z$. Obviously, the modal solutions of interest occur for $z = 0$, although viewing H more generally as a mapping facilitates the analysis below. For many waveguiding structures one must solve $H(k, \omega) = 0$ numerically, via a complex-plane root search, but for the CTLs of interest here an explicit solution can be obtained, $k_n(\omega) = (\pm) \frac{1}{\sqrt{2}} \sqrt{-T + \nu_n D}$, as given in (11).

The mapping $H(k, \omega) = z$ defines a surface in \mathbb{C}^2 , and for the simple case of $(k, \omega, z) \in \mathbb{R}$, this is depicted in Fig. 2. The particular case of $H(k, \omega) = 0$ defines a curve (solid line in Fig. 2), which is the dispersion curve of interest, and the smoothness of that curve at a given point determines important modal properties. In particular, one can define regular and singular points of the curve associated with certain modal behavior [20–23]. In the following we consider k as the unknown and ω as a

distinguished parameter, although the roles can also be reversed.

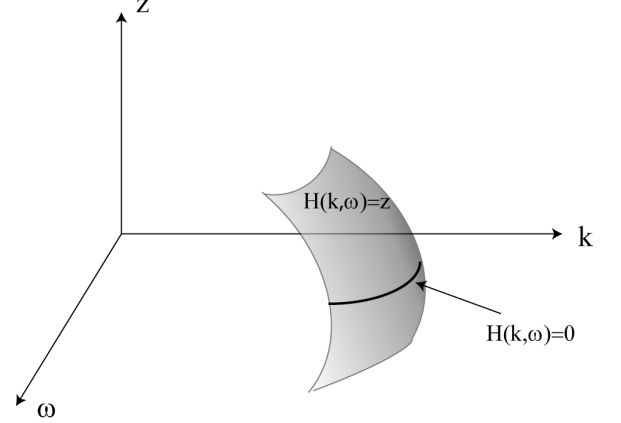


Figure 2. Depiction of the surface defined by $H(k, \omega) = z$, for $(k, \omega, z) \in \mathbb{R}$. The surface $H(k, \omega) = z$ may intersect the (k, ω) -plane, at $H(k, \omega) = 0$, resulting in the curved line of intersection shown that represents a standard dispersion diagram. If $H(k, \omega) = 0$ does not have solutions for $(k, \omega) \in \mathbb{R}$, then solutions can be found in complex space.

We first define a regular point on the curve $H(k, \omega) = 0$ as a point where $\partial H / \partial k \neq 0$. At a regular point the implicit function theorem [43] can be used to show that a unique smooth curve $k = k(\omega)$ exists in the neighborhood of the point. Except for a finite number of non-regular points (a set of measure zero), all points of modal dispersion are regular points, wherein the dispersion curve is smooth and single-valued. It is also worthwhile to note that differentiation $d/d\omega$ of $H(k, \omega) = 0$ leads to, via the chain rule,

$$\frac{dk}{d\omega} = -\frac{\partial H / \partial \omega}{\partial H / \partial k}, \quad (31)$$

and, therefore, at a regular point the tangent of $k(\omega)$ (related to the group velocity) is well-defined. However, of particular interest are the singular points [23] of the mapping H , which ultimately lead to branch points in the complex-frequency plane [21, 24]. The point (k_s, ω_s) is said to be a singular point of the mapping H if [42, p. 2]

$$H(k_s, \omega_s) = H'_k(k_s, \omega_s) = 0. \quad (32)$$

Obviously, in this case the tangent (31) is undefined. In [42, p. 45] it is shown that $H'_k(k_s, \omega_s) = 0$ is a necessary condition for the solution of $H(k_s, \omega_s) = 0$ to be a bifurcation point (a point where the number of solutions changes). For the two coupled transmission lines described above, Fig. 3 shows a plot of $H(k, \omega)$ in the vicinity of the EPD $(k_s, \omega_s) = (k_e, \omega_e)$ (the green, curved surface; numerical values of the CTL parameters are the same as given in Section II C). The intersection with the

zero plane (solid blue) is clearly visible, which forms the dispersion curve; the 2D dispersion is shown as the black solid line (see also Fig. 4a in [19]). A plot of the function $H'_k(k, \omega)$ is also shown in Fig. 3 (the slanted orange plane); units of $H(k, \omega)$ (green) and $H'_k(k, \omega)$ (pink) are in m^{-4} and m^{-3} , respectively. The intersection of $H'_k(k, \omega)$ with the $z = 0$ plane forms the line $H'_k(k, \omega) = 0$ shown in the figure with a black dashed curve. The intersection of $H(k, \omega)$ and $H'_k(k, \omega)$ on the $z = 0$ plane is at the singular point (EPD) denoted by a black solid circle (note that for $\omega < \omega_e$ the solid and dashed curves seem to overlap. This is merely due to the scale of the plot; the two lines actually only intersect at the EPD). For both H and H'_k the real part of the function is shown, as the imaginary parts are negligible.

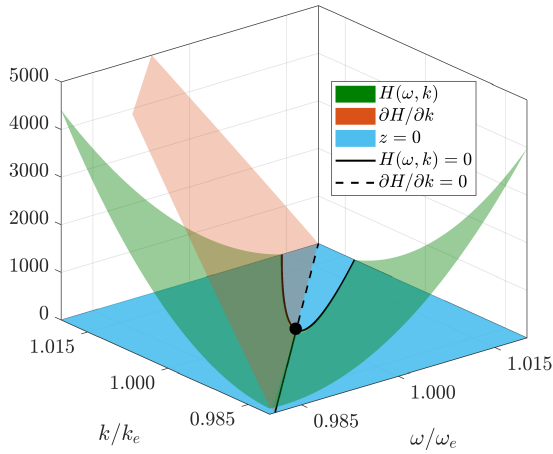


Figure 3. The functions $H(k, \omega)$ (green), $H'_k(k, \omega)$ (pink), and the zero plane (blue) vs. k, ω in the vicinity of the EPD (solid dot). The 2D dispersion $H(k, \omega) = 0$ is also shown (solid black line). The black dashed line is $H'_k(k, \omega) = 0$. Units of $H(k, \omega)$ (green) and $H'_k(k, \omega)$ (pink) are in m^{-4} and m^{-3} , respectively.

In addition to the conditions (32), we defined a fold bifurcation point (also known as a turning point, or limit point) when H satisfies (32) together with

$$H''_{kk}(k_s, \omega_s) \neq 0, \quad H'_\omega(k_s, \omega_s) \neq 0. \quad (33)$$

The zero conditions (32) together with the nonzero condition $H''_{kk}(k_s, \omega_s) \neq 0$ indicates that the degeneracy is of second-order, i.e., where two modal eigenvalues coalesce, as given in (21)-(22). The nonzero condition $H'_\omega(k_s, \omega_s) \neq 0$ serves as a sufficient condition for ω_s to be a BP in the complex ω -plane, as proved in [21] using the Weierstrass preparation theorem. In [20-23, 25, 44] the importance of fold singular points in modal interaction phenomena on guided-wave structures has been addressed in connection with the fold bifurcation from bifurcation theory [41, 42].

Notably, the zero and non-zero conditions (32)-(33) are the same as (21)-(22), and (27) that arise from linear algebra analysis. Thus, it can be concluded that the fold singular point considered in, e.g., [20-23, 25, 44] is in fact an EPD which may reside generally in the complex plane $(k, \omega) \in \mathbb{C}^2$. Therefore, in the following we denote (k_s, ω_s) as (k_e, ω_e) . An analogous treatment of EPDs using the conventional coupled-mode theory [45] is briefly outlined in the appendix.

Characteristic form. In the local neighborhood of the fold point (FP)/EPD (k_e, ω_e) the qualitative behavior of the mapping H can be represented by the normal form [41, p. 308-309], [42, p. 196-198],

$$\begin{aligned} (k - k_e)^2 + (\omega - \omega_e) &= 0, \quad \Delta > 0, \\ (k - k_e)^2 - (\omega - \omega_e) &= 0, \quad \Delta < 0 \end{aligned} \quad (34)$$

where $\Delta = H''_{kk}(k_e, \omega_e)H'_\omega(k_e, \omega_e)$, leading to the dispersion function

$$\begin{aligned} k(\omega) &= k_e \pm i\sqrt{\omega - \omega_e}, \quad \Delta > 0, \\ k(\omega) &= k_e \pm \sqrt{\omega - \omega_e}, \quad \Delta < 0. \end{aligned} \quad (35)$$

For the case of $\Delta > 0$ with $\omega < \omega_e$ two branching solutions $\Re(k(\omega))$ of $(k - k_e)^2 + (\omega - \omega_e)$ generate a parabola, and for $\omega > \omega_e$ two equal solutions $\Re(k(\omega))$ exist as a straight line $k(\omega) = k_e$. This corresponds to the characteristic intersection of a parabola and a straight line that occurs at a point of fold bifurcation [41, 42], as shown in Fig. 3 (see also [19]). When $\omega = \omega_e$ there is only one solution (k_e, ω_e) corresponding to the fold point. Also, $\Im(k(\omega))$ for $\omega < \omega_e$ yields the solution $k(\omega) = 0$, and for $\omega > \omega_e$ two branching solutions form a parabola in the imaginary plane of $k(\omega)$. A similar analysis can be applied to the case of $\Delta < 0$.

It should be noted that the conditions (32) and (33) define both real and complex FPs/EPDs, however, the normal form (34) is applicable for real valued FPs, where Δ is real-valued. Otherwise, the quantitative behavior of the local structure of the function $H(k, \omega)$ in the vicinity of FP/EPD can be obtained with a Taylor series expansion. Explicitly, the Taylor series in the vicinity of the EPD can be written as

$$\begin{aligned} H(k, \omega) &= H(k_e, \omega_e) + H'_k(k - k_e) + H'_\omega(\omega - \omega_e) \\ &+ \frac{1}{2}H''_{kk}(k - k_e)^2 + H''_{k\omega}(k - k_e)(\omega - \omega_e) \\ &+ \frac{1}{2}H''_{\omega\omega}(\omega - \omega_e)^2 + \dots = 0. \end{aligned} \quad (36)$$

Since $H(k_e, \omega_e) = H'_k(k_e, \omega_e) = 0$, and discarding the higher-order terms,

$$k - k_e \simeq \pm \alpha_1 (\omega - \omega_e)^{1/2} + \alpha_2 (\omega - \omega_e) \pm \alpha_3 (\omega - \omega_e)^{3/2} + O((\omega - \omega_e)^2) \quad (37)$$

where

$$\alpha_1 = \sqrt{-2 \frac{H''_{\omega\omega}}{H''_{kk}}}, \quad \alpha_2 = -\frac{H''_{k\omega}}{H''_{kk}}, \quad \alpha_3 = \frac{\alpha_1}{2} \frac{(H''_{\omega\omega})^2 - H''_{\omega\omega}H''_{kk}}{-2H''_{\omega\omega}H''_{kk}}. \quad (38)$$

The coefficient α_1 is the same as (25), and the higher-order coefficients are the same as given in [38] retaining the same order of terms.

C. EDPs leading to branch points in the complex-frequency plane

Regarding Statements 2 and 3, it is clear from several points of view that $D = 0$ defines a degeneracy in the eigenvalue plane, and a square-root-type BP in the complex-frequency plane (since $\mathbf{A} = \mathbf{A}(\omega)$ for $\mathbf{A} = -\underline{\mathbf{Z}}\underline{\mathbf{Y}}$, $-\underline{\mathbf{Y}}\underline{\mathbf{Z}}$, or $\underline{\mathbf{M}}$). Solving $D = 0$ leads to the frequency where the BP/EPD occurs (this also can be obtained by substituting $k^2 = -T/2$ from (13) into (14)). Assuming for simplicity that $\underline{\mathbf{G}} = \underline{\mathbf{0}}$, this leads to

$$\omega_e^2 a + \omega_e b + c = 0, \quad (39)$$

where, for $L_{11} = L_{22} = L$ and $C_{11} = C_{22} = C$ (C_{nm} is the nm th element of the capacitance matrix),

$$\begin{aligned} a &= 4(C_{12}L + CL_{12})^2, \\ b &= -4iC_{12}(CL_{12} + LC_{12})(R_{11} + R_{22}), \\ c &= -2R_{22}R_{11}(2C_{12}^2 - C^2) - C^2(R_{11}^2 + R_{22}^2). \end{aligned} \quad (40)$$

If $(R_{11} + R_{22}) \neq 0$, then ω_e will not be on the real- ω axis, assuming $(CL_{12} + LC_{12}) \neq 0$.

For the PT-symmetric case, $R_{11} = -R = -R_{22}$,

$$\omega_e = \sqrt{\frac{-c}{a}} = R \frac{\sqrt{C^2 - C_{12}^2}}{C_{12}L + CL_{12}}. \quad (41)$$

This will occur on the real- ω axis, since one expects $C^2 > C_{12}^2$, proving Statement 4. Note that from a design point of view, expression (41) leads to the needed value of R for a desired value of ω_e .

If we assume that $\underline{\mathbf{G}} \neq \underline{\mathbf{0}}$, for $L_{11} = L_{22} = L$, $C_{11} = C_{22} = C$, and the PT-symmetric case, $R_{11} = -R = -R_{22}$ and $G_{11} = -G = -G_{22}$,

$$\omega_e^2 = -\frac{G^2L_{12}^2 + R^2C_{12}^2 - X - (G^2L^2 + C^2R^2)}{(CL_{12} + LC_{12})^2}$$

where $X = 2GR(LC + C_{12}L_{12})$. If $R = 0$,

$$\omega_e = \frac{G\sqrt{L^2 - L_{12}^2}}{C_{12}L + CL_{12}} \quad (42)$$

which is the dual of (41).

As an example, Fig. 4 shows $\Im(k/k_e)$ versus $\Re(k/k_e)$ in the vicinity of the fold point for numerical parameters taken from [19] corresponding to two coupled microstrip lines (strip width 3 mm, gap between strips 0.1 mm; substrate height 0.75 mm, and dielectric constant of 2.2); $C_{11} = C_{22} = C = 0.12$ nF/m, $L_{11} = L_{22} = L = 0.18$ μ H/m, $L_{12} = L_{21} = 49.24$ nH/m, $C_{12} = C_{21} = -25.83$ pF/m, and $\underline{\mathbf{G}} = \underline{\mathbf{0}}$. Setting a target frequency of

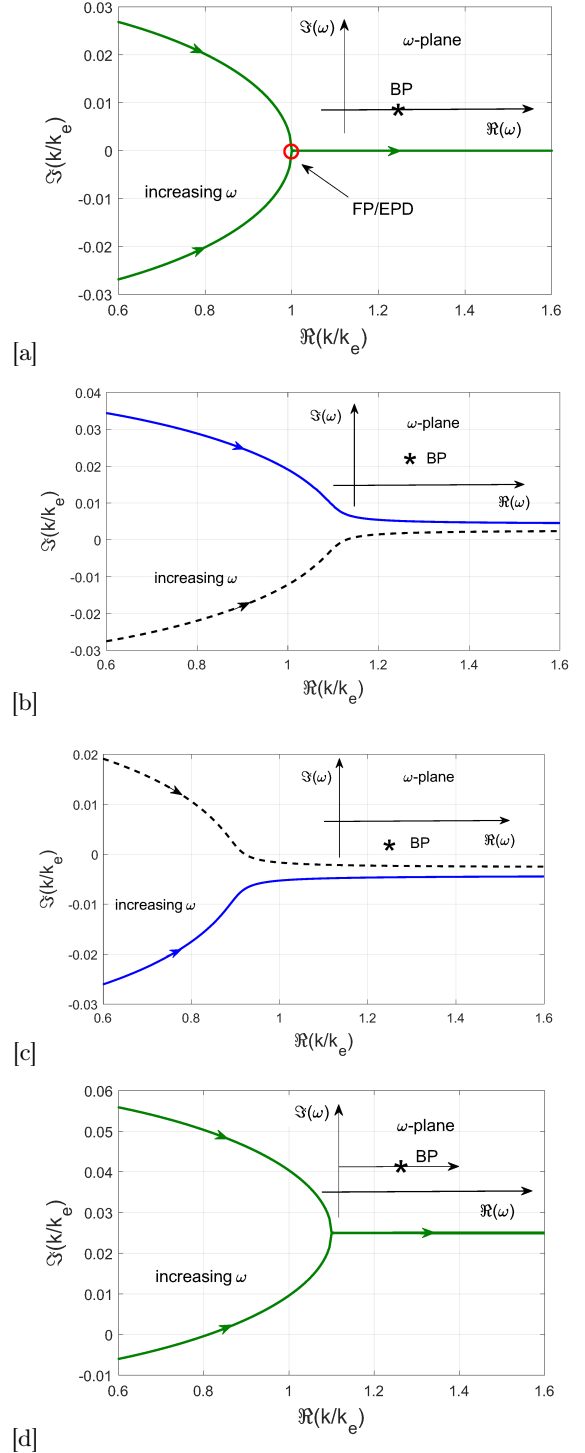


Figure 4. Dispersion behavior near an EPD for coupled transmission lines with (a) $R_{11} = -R_{22} = -73.172$ ohms (PT-symmetric case), as ω varies from $0.5\omega_e$ to $1.5\omega_e$ along the real- ω axis. (b) Same as (a) but for $R_{11} = -1.2R_{22}$, where the EPD lies above the real-frequency axis. (c) Same as (a) but for $R_{11} = -0.8R_{22}$, such that the EPD is below the real-frequency axis. (d) Same as (b) but for $\Re(\omega)$ varying from $0.5\omega_e$ to $1.5\omega_e$ at a constant value $\Im(\omega) = \Im(\omega_s) = (0.022\omega_e)$. In all cases the pair (k_e, ω_e) are the values at PT-symmetry, $(k_e, \omega_e) = (28.649 \text{ m}^{-1}, 2\pi 10^9 \text{ s}^{-1})$, $R_{22} = 73.172$ ohms, and the star indicates the BP/EPD.

$\omega_e = 2\pi 10^9 \text{ s}^{-1}$, from (41), to place the EPD on the real frequency axis at ω_e requires $R_{11} = -R_{22} = -73.172$ ohms. The corresponding value of wavenumber at the EPD is $k_e = 28.649 \text{ m}^{-1}$. A two-dimensional root search of (32)-(33) yields $(k_s/k_e, \omega_s/\omega_e) = (1, 1)$ as expected. Dispersion behavior in the vicinity of the fold point is shown in Fig. 4a.

For other values of $R_{11} = -R_{22}$ (i.e., maintaining PT-symmetry) the fold point remains on the $\Re(\omega)$ axis, but moves to lower or higher frequencies as indicated in (41). Upon breaking PT-symmetry by using $R_{11} \neq -R_{22}$, the BP/EPD does not occur on the real-frequency axis, as shown in Figs. 4b,c,d, where in all cases $R_{22} = 73.172$ ohms. For $R_{11} = -1.2R_{22}$ the 2D root search of (32)-(33) yields $(k_s/k_e, \omega_s/\omega_e) = (1.1 + i0.025, 1.1 + i0.022)$, where (k_e, ω_e) are the values given above under the PT-symmetry conditions, $(k_e, \omega_e) = (28.649 \text{ m}^{-1}, 2\pi 10^9 \text{ s}^{-1})$. As such, the EPD lies above the real-frequency axis, and Fig. 4b shows the corresponding dispersion behavior. Since a scanning of an operating frequency (assumed real) does not pass through the branch point, the eigenvalues do not become degenerate. Alternatively, Fig. 4c shows the dispersion behavior when $R_{11} = -0.8R_{22}$, such that the EPD is below the real-frequency axis and the modes have interchanged with their counterparts in Fig. 4b. Fig. 4d shows the dispersion behavior for the case $R_{11} = -1.2R_{22}$, when the real part of frequency is varied while keeping a constant $\Im(\omega) = \Im(\omega_s) = (0.022\omega_e)$, and so passing through the singular point (EPD), at which point the modal degeneracy is recovered at a complex-valued k . In this complex frequency case a BP is clearly visible and occurs at a complex value wavenumber. Regarding Figs. 4b,c, note that to interchange the modal solutions it is not necessarily to encircle the EPD/BP (as done in, for example [7], [46]). It is shown in Figs. 4b,c that the interchange of solutions is due to varying the frequency path above or below the BP [24, 28].

III. CONCLUSIONS

We have examined several aspects of EPDs on two coupled transmission lines, demonstrating that in the framework of the eigenvalue problem the eigenvalue degeneracies are always coincident with eigenvector degeneracies, such that all eigenvalue degeneracies correspond to EPDs. We also discussed the fact that EPDs are related to branch-point singularities in the complex-frequency plane, as can be ascertained from both linear algebra concepts and from the theory of singular points of complex mappings and bifurcation theory. Moreover, we have provided a connection between the linear algebra approach and an approach based on singularity and bifurcation theories, previously used to study modal interactions on guided-wave structures. We have presented simple closed-form expressions for the complex-frequency plane EPDs, and showed that under PT-symmetry these branch points reside on the real-frequency axis and gener-

alized the branch point discussion to complex frequency and wavenumbers.

ACKNOWLEDGMENTS

This material is based upon M.O and F.C work supported by the Air Force Office of Scientific Research under award number FA9550-15-1-0280.

APPENDIX: COUPLED-MODE THEORY

In addition to the transmission-line treatment of EPDs, here we briefly comment on the matrix that arises from conventional so called ‘‘coupled-mode theory’’ [45]. For simplicity, we consider the PT-symmetric case for otherwise identical individual transmission lines (e.g., one will have loss and one will have gain). Then, the individual (uncoupled) lines have propagation constants β and β^* , which, when brought into proximity, become $\beta + \delta$ and $\beta^* + \delta^*$ under the coupling constant κ . The coupled system modes obey the evolution equation [47]

$$i \frac{d}{dz} \begin{bmatrix} a_1 \\ a_2 \end{bmatrix} = \begin{bmatrix} \beta + \delta & \kappa \\ \kappa^* & (\beta + \delta)^* \end{bmatrix} \begin{bmatrix} a_1 \\ a_2 \end{bmatrix} = \underline{\underline{\beta}} \begin{bmatrix} a_1 \\ a_2 \end{bmatrix} \quad (43)$$

where a_1 and a_2 are the wave amplitudes in transmission lines 1 and 2, respectively. One can proceed with examination of the eigenvectors and eigenvalues, but it suffices to consider, analogous to (18), the dispersion relation

$$H(k, \omega) = \left| \begin{bmatrix} \beta(\omega) + \delta(\omega) & \kappa(\omega) \\ \kappa^*(\omega) & (\beta(\omega) + \delta(\omega))^* \end{bmatrix} - k \begin{bmatrix} 1 & 0 \\ 0 & 1 \end{bmatrix} \right| = 0 \\ = k^2 - k \text{Tr}(\underline{\underline{\beta}}) + \det(\underline{\underline{\beta}}) = 0 \quad (44)$$

where $\underline{\underline{\beta}}$ is the 2×2 matrix in (43). Obviously, (44) is analogous to (19). Furthermore,

$$H'_k(k, \omega) = 2k - (\beta^* + \delta^* + \beta + \delta) = 0 \quad (45)$$

leads to

$$k = \frac{1}{2} (\beta^* + \delta^* + \beta + \delta) = \Re(\beta + \delta) = \frac{1}{2} \text{Tr}(\underline{\underline{\beta}}) \quad (46)$$

and using (44) one obtains

$$\text{Tr}^2(\underline{\underline{\beta}}(\omega)) - 4 \det(\underline{\underline{\beta}}(\omega)) = 0 \quad (47)$$

which is the condition $D = 0$ in (8), and which leads to the value of the EPD frequency $\omega = \omega_e$. The nonzero condition $H'_\omega(k, \omega) \neq 0$ can be evaluated if all matrix entries are known as a function of frequency. Thus, coupled-mode theory leads to the same analysis of EPDs as the CTL formulation presented in Section II, and, therefore, can also be analyzed using bifurcation theory.

-
- [1] W. D. Heiss, *The physics of exceptional points*, J. Phys. Math. Theor. **45**, 444016, 2012.
 - [2] C. M. Bender and S. Boettcher, *Real spectra in non-Hermitian Hamiltonians having PT symmetry*, Phys. Rev. Lett. **80**, 5243, 1998.
 - [3] C. M. Bender, S. Boettcher, and P. N. Meisinger, *PT-symmetric quantum mechanics*, J. Math. Phys. **40**, 2201, May 1999.
 - [4] C. E. Rüter, K. G. Markis, R. El-Ganainy, D. N. Christodoulides, M. Segev, and D. Kip, *Observation of parity-time symmetry in optics*, Nature Phys. **6**, 192, Mar. 2010.
 - [5] H. Hodaei, M. A. Miri, A. U. Hassan, W. E. Hayenga, M. Heinrich, D. N. Christodoulides, and M. Khajavikhan, *Parity-time-symmetric coupled microring lasers operating around an exceptional point*, Opt. Lett. **40**, 4955, Nov. 2015.
 - [6] M. A. K. Othman, V. Galdi, and F. Capolino, *Exceptional points of degeneracy and PT symmetry in photonic coupled chains of scatterers*, Phys. Rev. B **95**, 104305, 2017.
 - [7] A. U. Hassan, B. Zhen, M. Soljačić, M. Khajavikhan, and D. N. Christodoulides, *Dynamically encircling exceptional points: Exact evolution and polarization state conversion*, Phys. Rev. Lett. **118**, 093002, 2017.
 - [8] D. L. Sounas, R. Fleury, and A. Alù, *Unidirectional cloaking based on metasurfaces with balanced loss and gain*, Phys. Rev. Appl. **4**, 014005, 2015.
 - [9] F. Monticone, C. A. Valagiannopoulos, and A. Alù, *Parity-time symmetric nonlocal metasurfaces: All-angle negative refraction and volumetric imaging*, Phys. Rev. X **6**, 041018, 2016.
 - [10] C. A. Valagiannopoulos, F. Monticone, and A. Alù, *PT-symmetric planar devices for field transformation and imaging*, J. Opt. **18**, 044028, 2016.
 - [11] M. Sakhdari, M. Farhat, and P.-Y. Chen, *PT-symmetric metasurfaces: Wave manipulation and sensing using singular points*, New J. Phys. **19**, 065002, 2017.
 - [12] T. Kato, *Perturbation Theory for Linear Operators*, Springer-Verlag, Berlin, 1995.
 - [13] A. Figotin and I. Vitebskiy, *Frozen light in photonic crystals with degenerate band edge*, Phys. Rev. E **74**, 066613, 2006.
 - [14] A. Figotin and I. Vitebskiy, *Slow-wave resonance in periodic stacks of anisotropic layers*, Phys. Rev. A **76**, 053839, 2007.
 - [15] M. A. K. Othman, F. Yazdi, A. Figotin, F. Capolino, *Giant gain enhancement in photonic crystals with a degenerate band edge*, Phys. Rev. B **93**, 024301, 2016.
 - [16] J. L. Volakis and K. Sertel, *Narrowband and wideband metamaterial antennas based on degenerate band edge and magnetic photonic crystals*, Proc. IEEE **99**, 1732, 2011.
 - [17] E. Hernández, A. Jáuregui, A. Mondragón, and L. Nellen, *Degeneracy of resonances: Branch point and branch cuts in parameter space*, Int. J. Theor. Phys. **46**, 1666, 2007.
 - [18] E. Hernández, A. Jáuregui, and A. Mondragón, *Exceptional points and non-Hermitian degeneracy of resonances in a two-channel model*, Phys. Rev. E **84**, 046209, 2011.
 - [19] M.A.K. Othman and F. Capolino, *Theory of exceptional points of degeneracy in uniform coupled waveguides and balance of gain and loss*, IEEE Trans. Ant. Propag. **21**, 5289, 2017.
 - [20] A. B. Yakovlev and G. W. Hanson, *On the nature of critical points in leakage regimes of a conductor backed coplanar strip line*, IEEE Trans. Microwave Theory Tech. **45**, 87, 1997.
 - [21] G. W. Hanson and A. B. Yakovlev, *An analysis of leaky-wave dispersion phenomena in the vicinity of cutoff using complex frequency-plane singularities*, Radio Science **33**, 803, 1998.
 - [22] A. B. Yakovlev and G. W. Hanson, *Analysis of mode coupling on guided-wave structures using Morse critical points*, IEEE Trans. Microwave Theory Tech. **46**, 966, 1998.
 - [23] A. B. Yakovlev and G. W. Hanson, *Fundamental modal phenomena on isotropic and anisotropic planar slab dielectric waveguides*, IEEE Trans. Antennas Propag. **51**, 888, 2003.
 - [24] G. W. Hanson and A. B. Yakovlev, *Investigation of mode interaction on planar dielectric waveguides with loss and gain*, Radio Science **34**, 1349, 1999.
 - [25] A. B. Yakovlev and G. W. Hanson, *Mode transformation and mode continuation regimes on waveguiding structures*, IEEE Trans. Microwave Theory Tech. **48**, 67, 2000.
 - [26] G. Lovat, P. Burghignoli, A. B. Yakovlev, and G. W. Hanson, *Modal interactions in resonant metamaterial slabs with losses*, Metamaterials **2**, 198, 2008.
 - [27] A. B. Yakovlev and G. W. Hanson, *Modal propagation and interaction in the smooth transition from a metal mushroom structure to a bed-of-nails-type wire media*, J. Appl. Phys. **111**, 074308, 2012.
 - [28] G. W. Hanson, A. B. Yakovlev, and J. Hao, *Leaky-wave analysis of transient fields due to sources in planarly-layered media*, IEEE Trans. Antennas Propag. **51**, 146, 2003.
 - [29] C. R. Paul, *Analysis of Multiconductor Transmission Lines*, Hoboken, NJ, USA: Wiley, 2008.
 - [30] G. Miano and A. Maffucci, *Transmission Lines and Lumped Circuits: Fundamentals and Applications*, San Francisco, CA, USA: Academic, 2001.
 - [31] R. F. Harrington, *Time-Harmonic Electromagnetic Fields*, Ch. 8, McGraw-Hill, 1961.
 - [32] M. A. K. Othman, V. A. Tamma, and F. Capolino, *Theory and new amplification regime in periodic multimodal slow wave structures with degeneracy interacting with an electron beam.* IEEE Trans. Plasma Sci. **44**, 594, 2016.
 - [33] D. G. Baranov, A. Krasnok, and A. Alù, *Coherent virtual absorption based on complex zero excitation for ideal light capturing*, Optica, in press.
 - [34] C. E. Baum, *Emerging technology for transient and broad-band analysis and synthesis of antennas and scatterers*, Proc. IEEE **64**, 1598, 1976.
 - [35] C. E. Baum, *The Singularity Expansion Method*, in Transient Electromagnetic Fields, L. B. Felsen, Ed. New York Springer-Verlag, 128, 1976.
 - [36] For uncoupled, non-identical lines ($Z_{12} = Y_{12} = 0$ and $Z_{11} = Z_{22} = Z$, $Y_{11} = Y_{22} = Y$), $k_1 = \pm\sqrt{-Y_{11}Z_{11}}$, $k_2 = \pm\sqrt{-Y_{22}Z_{22}}$ and $m(k) = l(k) = 2$.

- [37] P. Lancaster and M. Tismenetsky, *The Theory of Matrices*, 2nd Ed., Academic Press, 1985.
- [38] A. Welters, *On explicit recursive formulas in the spectral perturbation analysis of a Jordan block*, SIAM J. Matrix Anal. Appl. **32**, 1, pp. 1–22, 2011.
- [39] C. D. Meyer, *Matrix Analysis and Applied Linear Algebra* (SIAM, Philadelphia, 2000). Ch. 8.
- [40] G.W. Hanson, A.I. Nosich, and E.M. Kartchevski, *Green's function expansions in dyadic root functions for shielded layered waveguide problems obtained via residue theory*, Progress in Electromagnetics Research, PIER 39, pp. 61-91, 2003.
- [41] R. Seydel, *Practical Bifurcation and Stability Analysis*, 2nd ed., New York: Springer-Verlag, 1994.
- [42] M. Golubitsky and D. G. Schaeffer, *Singularities and Groups in Bifurcation Theory*, Berlin: Springer-Verlag, 1985, vol. 1.
- [43] T. Poston and I. Stewart, *Catastrophe Theory and Its Applications*, London, U.K.: Sir Isaac Pitman, 1978.
- [44] A. B. Yakovlev and G. W. Hanson, *Fundamental wave phenomena on biased-ferrite planar slab waveguides in connection with singularity theory*, IEEE Trans. Microwave Theory Tech. **51**, 583, 2003.
- [45] H. Haus, W. Huang, S. Kawakami, N. Whitaker, *Coupled-mode theory of optical waveguides*, J. Lightwave Technology **5**, 16, 1987.
- [46] J. Doppler, A. A. Mailybaev, J. Böhm, U. Kuhl, A. Girschik, F. Libisch, T. J. Milburn, P. Rabl, N. Moiseyev and S. Rotter, *Dynamically encircling an exceptional point for asymmetric mode switching*, Nature **537**, 76, 2016.
- [47] A. Guo, G. J. Salamo, D. Duchesne, R. Morandotti, M. Volatier-Ravat, V. Aimez, G. A. Siviloglou, and D. N. Christodoulides, *Observation of PT-symmetry breaking in complex optical potentials*, Phys Rev. Lett. **103**, 093902, 2009.